

SCIENTIFIC REPORTS



OPEN

Effect of BI-1 on insulin resistance through regulation of CYP2E1

Geum-Hwa Lee^{1,*}, Kyoung-Jin Oh^{2,3,*}, Hyung-Ryong Kim^{4,*}, Hye-Sook Han², Hwa-Young Lee¹, Keun-Gyu Park⁵, Ki-Hoan Nam⁶, Seung-Hoi Koo² & Han-Jung Chae¹

Received: 04 August 2015

Accepted: 04 August 2016

Published: 31 August 2016

Diet-induced obesity is a major contributing factor to the progression of hepatic insulin resistance. Increased free fatty acids in liver enhances endoplasmic reticulum (ER) stress and production of reactive oxygen species (ROS), both are directly responsible for dysregulation of hepatic insulin signaling. BI-1, a recently studied ER stress regulator, was examined to investigate its association with ER stress and ROS in insulin resistance models. To induce obesity and insulin resistance, BI-1 wild type and BI-1 knock-out mice were fed a high-fat diet for 8 weeks. The BI-1 knock-out mice had hyperglycemia, was associated with impaired glucose and insulin tolerance under high-fat diet conditions. Increased activity of NADPH-dependent CYP reductase-associated cytochrome p450 2E1 (CYP2E1) and exacerbation of ER stress in the livers of BI-1 knock-out mice was also observed. Conversely, stable expression of BI-1 in HepG2 hepatocytes was shown to reduce palmitate-induced ER stress and CYP2E1-dependent ROS production, resulting in the preservation of intact insulin signaling. Stable expression of CYP2E1 led to increased ROS production and dysregulation of insulin signaling in hepatic cells, mimicking palmitate-mediated hepatic insulin resistance. We propose that BI-1 protects against obesity-induced hepatic insulin resistance by regulating CYP2E1 activity and ROS production.

Anti-apoptotic protein Bax inhibitor-1 (BI-1) protects against apoptosis induced by ER stress^{1–3}. In previous BI-1 studies, reactive oxygen species (ROS) regulation characteristics have been investigated^{2,4}. In ER, the major source of ROS is the microsomal monooxygenase system. Although the main function of the microsomal monooxygenase system is to oxygenate exogenous compounds (xenobiotics) and some endogenous substrates, the microsomal monooxygenase system also produces reactive oxygen species (ROS), such as superoxide anion radical and H₂O₂^{5–7}. The efficiency, or degree of coupling, of electron transfer from NADPH to CYP is usually <50–60%, and is often as low as 0.5–3.0%. This ‘electron leakage’ contributes significantly to ROS production during redox cycling between NADPH-cytochrome CYP reductase (CPR) and eukaryotic CYPs. ROS production is increased by electron leakage from ER stress-associated CYP2E1 activation, which itself is inhibited by BI-1 overexpression⁸.

The inhibitory effect of BI-1 on ROS production has been primarily linked to cell protection mechanisms. Although direct association with the ER stress signaling pathway has not been formally established, an abundance of ROS often coincides with insulin resistance^{9–11}. Increased hepatic CYP2E1 protein expression and activity in association with enhanced ROS generation have recently been reported in animal models of obesity and in patients with obesity and both alcoholic and nonalcoholic fatty liver disease^{12,13}. These results suggest a role for increased ROS generation in the pathogenesis of insulin resistance.

Insulin resistance consists of a cluster of metabolic disorders. Hepatic lipid accumulation is strongly associated with insulin resistance¹¹, and it is widely accepted that lipid accumulation represents the hepatic manifestations of systemic impairments in the insulin network. Insulin resistance studies have demonstrated that phosphorylation of IRS1/2 is controlled by JNK (c-Jun N-terminal kinase) phosphorylation as a signal transduction mechanism^{14–16}. It has also been suggested that elevated ROS levels impair insulin signaling by way of several complex

¹Department of Pharmacology and New Drug Development Institute, Medical School, Chonbuk National University, Jeonju, 561-181, Republic of Korea. ²Division of Life Sciences, Korea University, 145 Anam-Ro, Seongbuk-Gu, Seoul, 136-713, Republic of Korea. ³Metabolic Regulation Research Center, Korea Research Institute of Bioscience and Biotechnology (KRIBB), Daejeon, 305-806, Republic of Korea. ⁴Department of Dental Pharmacology and Wonkwang Dental Research Institute, School of Dentistry, Wonkwang University, Iksan, 570-749, Republic of Korea. ⁵Department of Internal Medicine, Kyungpook National University School of Medicine, Daegu, 700-721, Republic of Korea. ⁶Laboratory Animal Resource Center, KRIBB, Ochang-eup, 363-883, Republic of Korea. *These authors contributed equally to this work. Correspondence and requests for materials should be addressed to S.-H.K. (email: koohei@korea.ac.kr) or H.-J.C. (email: hjchae@jbnu.ac.kr)

mechanisms, including phosphorylation of JNK and the subsequent downstream serine/threonine phosphorylation of IRS1^{17,18}. Elevation of ROS levels has been proposed as a link between free fatty acid and hepatic insulin resistance¹⁹. In this study, we hypothesized that palmitate-induced ER stress results in the accumulation of ROS, originating from the microsomal monooxygenase system in liver cells. We evaluated the role of BI-1 in the microsomal monooxygenase system and linked its activity to regulation of insulin resistance in liver cells and animal models.

Results

BI-1 knock-out disrupts insulin signaling and nutrient metabolism. To explore the role of BI-1 in glucose metabolism, glucose and insulin tolerance tests were first performed in normal diet-fed BI-1 wild-type and BI-1 knock-out mice. The results have shown no differences between wild-type and BI-1 knock-out mice, suggesting that BI-1 may not significantly affect glycemia under normal conditions (Fig. S1). To promote diet-induced obesity and insulin resistance, BI-1 wild-type and BI-1 knock-out mice were fed a high-fat diet for 8 weeks. Unlike the normal chow diet-fed conditions, the high fat diet-fed BI-1 knock-out mice exhibited higher plasma glucose levels than wild-type mice (Fig. 1a). No difference in body weight was noted between the two groups (Fig. 1b). Systemic depletion of BI-1 promoted both glucose and insulin intolerance in mice (Fig. 1c,d), and there were no major changes in plasma levels of insulin, triglyceride, and non-essential fatty acid or in hepatic lipid accumulation patterns (Fig. S2a,b). Western blot was performed to verify the integrity of hepatic insulin signaling. Diminished tyrosine phosphorylation of the insulin receptor (IR) and serine 473 phosphorylation of AKT was observed (Fig. 1e). Reduced phospho-FoxO1/FoxO1 ratio was noted in the livers of BI-1 knock-out mice, compared with control mice. Indeed, mRNA levels for genes responsible for gluconeogenesis (Glucose-6-phosphate translocase, Phosphoenolpyruvate carboxykinase, and proliferator-activated receptor- γ coactivator 1 α) were higher in the livers of BI-1 knock-out mice than in those of control mice, supporting our hypothesis (Fig. S3).

Despite impaired insulin signaling, elevated mRNA levels of genes involved in fatty acid synthesis (Sterol regulatory element-binding transcription factor 1c, fatty acid synthase, and acetyl-CoA carboxylase) was observed in BI-1 knock-out mice (Fig. S4a), consistent with the mixed insulin resistance phenotype that is often observed in models of type 2 diabetes²⁰. Simultaneous induction of genes responsible for triglyceride hydrolysis (hormone-sensitive lipase and adipose triglyceride lipase) and fatty acid beta oxidation (carnitine palmitoyltransferase 1a, medium chain acyl-CoA dehydrogenase, and acyl-CoA oxidase 1) was also observed, suggesting that BI-1 depletion invoked a futile cycle of fat synthesis, hydrolysis, and breakdown in the liver (Fig. S4b,c). There were no significant differences in hepatic expression of genes encoding proinflammatory cytokines between BI-1 wild-type and BI-1 knock-out mice (Fig. S5). No overall differences were observed with respect to food intake and physical activity between BI-1 wild-type and knock-out mice, suggesting that the observed phenotype in BI-1 knock-out mice may not be related to an alteration in overall energy metabolism (Fig. S6).

BI-1 ameliorates ER stress and its associated CYP2E1 activity and ROS accumulation. CYP2E1 has been suggested to mediate ER stress-associated ROS generation^{10,21,22}. First, increased protein level of CYP2E1 was found in the livers of BI-1 knock-out mice as compared with control mice (Fig. 2a), leading to an increased association with CPR (Fig. 2b). The increased interaction between CYP2E1 and CPR resulted in higher activity of CYP2E1 (Fig. 2c), as well as significant activation of lipid peroxidation in the livers of BI-1 knock-out mice (Fig. 2d), indicating increased ROS generation. Furthermore, the expression of Bip/GRP78, CHOP, phospho-PERK, phospho-eIF-2 α and phospho-IRE-1 α and its downstream spliced XBP-1 was more enhanced in the livers of BI-1 knock-out mice (Fig. 2e), also showing the recently established role of BI-1, an ER stress regulator.

Expression of BI-1 regulates insulin signaling and nutrient metabolism through a CYP2E1 and ER stress-associated mechanism.

First, adenovirus was injected into normal chow diet-fed mice. Glucose and insulin tolerance did not differ between mice expressing either control GFP or BI-1 (Fig. S7a). On the other hand, hepatic expression of BI-1 ameliorated both glucose and insulin intolerance in high fat diet-fed mice (Fig. 3a). High fat diet-mice expressing BI-1 also displayed reduced fasting blood glucose levels (Fig. 3b) without changes in body weight compared with GFP-expressing high fat diet-fed mice (Figs 3c and S8). Concomitant with changes in blood glucose levels, BI-1 expression in the liver of high fat diet-fed mice reduced plasma insulin levels (Fig. 3d). Both plasma and hepatic TG levels were significantly increased by high fat diet feeding, which was restored to normal levels by hepatic BI-1 expression (Fig. 3e,f). Consistent with this data, H&E staining revealed reduced lipid content in the livers of BI-1-expressing mice compared with controls (Fig. S9). As expected, significant increases in the expression of IL-1 β , IL-6, and MCP-1 were observed in those fed a high fat diet compared with controls fed a normal chow diet (Figs 3g and S10). The plasma levels of IL-1 β , IL-6, and MCP-1 were all reduced in BI-1-expressing mice compared with controls (Fig. 3g). Furthermore, BI-1 expression also improved insulin signaling in the livers of high fat diet-fed mice, as evidenced by increased tyrosine phosphorylation of IR, IRS-1, and IRS-2, and increased Akt phosphorylation compared with controls (Fig. 4a,b). Serine phosphorylations of IRS-1 and IRS-2 are considered negative feedback markers that inhibit insulin signaling. Significant increases in the serine phosphorylation of both IRS-1 and IRS-2 were observed upon high fat diet-feeding. These levels decreased to nearly normal levels with BI-1 expression.

Protein levels of hepatic CYP2E1 were also reduced in BI-1-overexpressing mice, leading to a decreased association with CPR (Fig. 4c,d). CYP2E1 activity and related lipid peroxidation in the livers of BI-1-overexpressing mice were significantly decreased (Fig. 4e,f). Accordingly, we observed decreased ER stress signaling in BI-1-expressing livers, suggesting the amelioration of ER stress conditions (Fig. 4g).

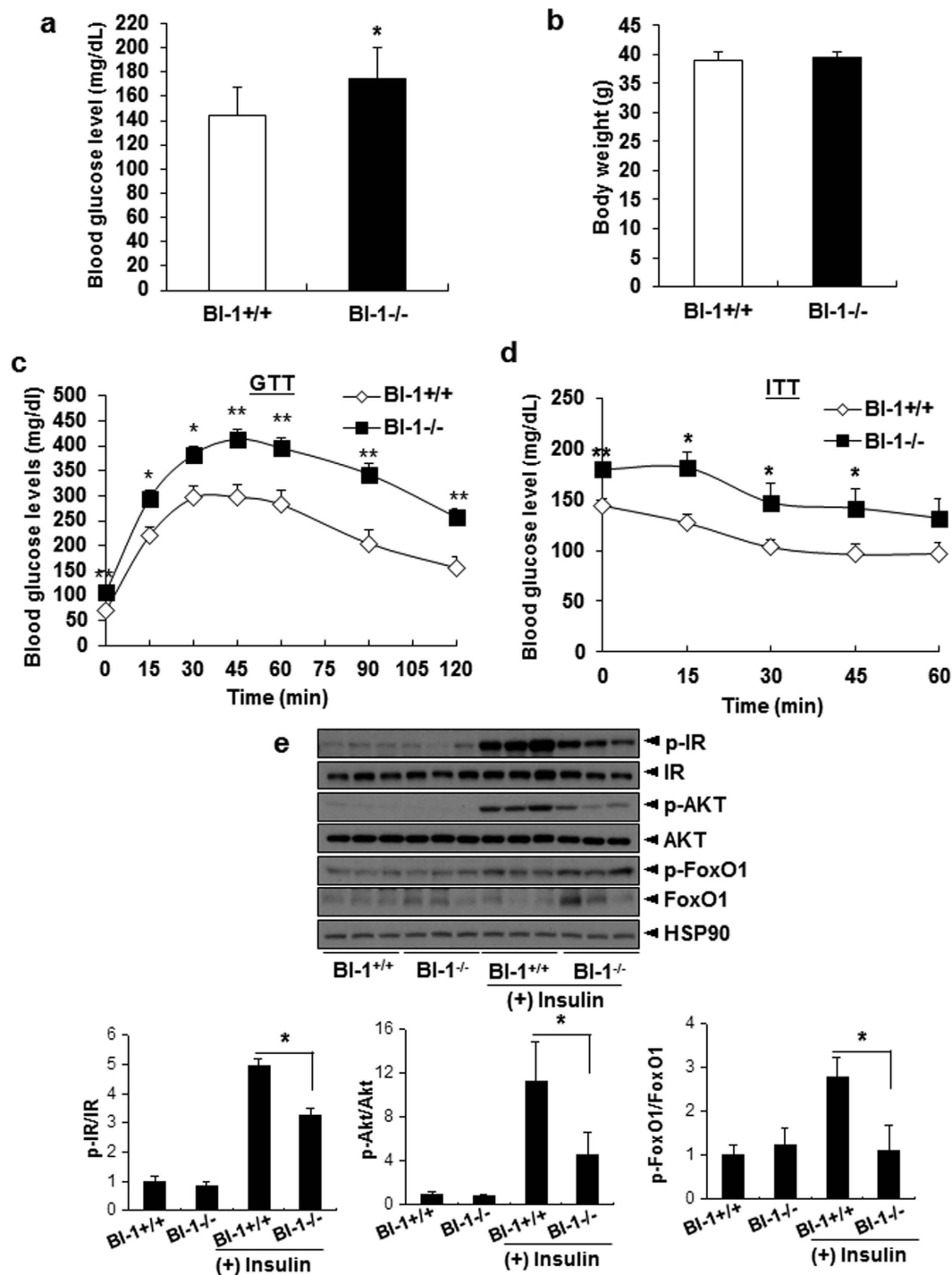


Figure 1. Chronic depletion of BI-1 impairs hepatic glucose metabolism and insulin signaling under high-fat diet conditions. (a) Body weight of BI-1 wild-type (BI-1^{+/+}) ($n = 10$) and BI-1 knock-out (BI-1^{-/-}) male mice ($n = 11$) fed high-fat diet for 8 weeks. (b) 6h fasting glucose levels of high-fat diet-fed mice. (c) Glucose tolerance test showing effects of chronic BI-1 depletion on glucose homeostasis. (d) Insulin tolerance test showing effects of BI-1 knock-out on insulin sensitivity. (e) Western blot analysis showing effects of chronic BI-1 depletion on insulin signaling pathway. Data in (a) through (d,e) represent mean \pm SEM (* $p < 0.05$, ** $p < 0.005$, *** $p < 0.0005$, t -test).

BI-1 regulates palmitate-induced insulin resistance through ER stress and associated CYP2E1 activity. Having observed the effect of BI-1 depletion on hepatic signaling *in vivo*, we next examined whether expression of BI-1 could induce the similar signaling cascades in cultured hepatocytes. A stable HepG2 hepatic cell line expressing BI-1 (BI-1 cells) and control cells (Neo cells) were generated, and cells were treated with

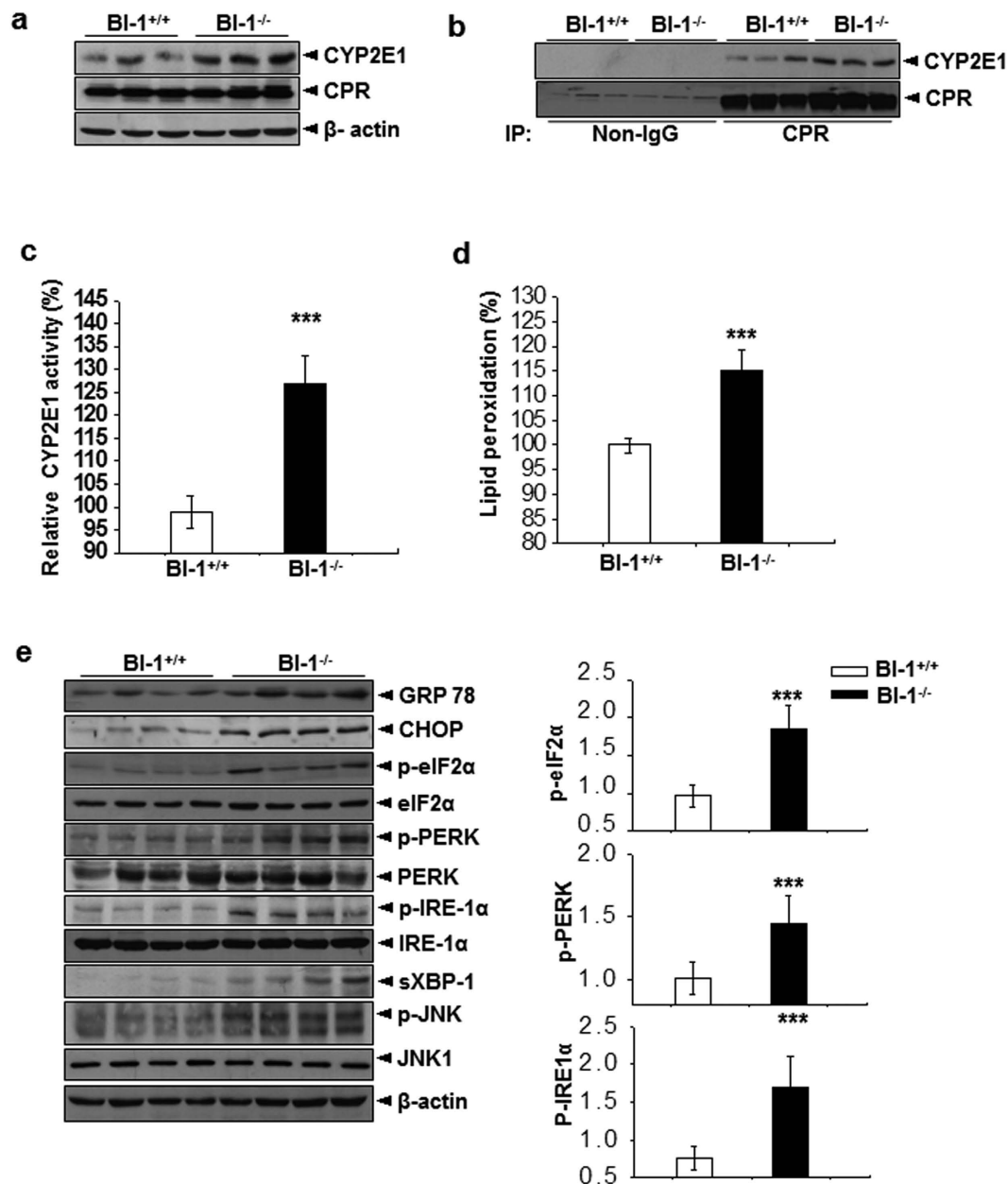


Figure 2. Chronic depletion of BI-1 increases hepatic CYP2E1 activity and promotes hepatic ER stress and ROS accumulation in high-fat diet-fed mice. (a) Western blot analysis showing effects of BI-1 depletion on expression levels of CYP2E1 and CPR in livers of BI-1 wild-type (BI-1^{+/+}) ($n = 5$) and BI-1 knock-out (BI-1^{-/-}) ($n = 5$) mice. (b) Co-immunoprecipitation assay of interaction between CPR and CYP2E1 in livers of BI-1 wild-type and BI-1 knock-out mice. (c) Estimation of chlorozoxane hydroxylase activity of CYP2E1 and (d) lipid peroxidation showing ER-stress induced ROS production in livers of BI-1 wild-type (BI-1^{+/+}) ($n = 5$) and BI-1 knock-out (BI-1^{-/-}) ($n = 5$) mice. (e) Western blot analysis showing effects of chronic depletion of BI-1 on ER stress signaling pathways in livers of high-fat diet-fed mice. Data in (c–e) represent mean \pm SD ($*p < 0.05$, $**p < 0.005$, $***p < 0.0005$, t -test).

palmitate. Phosphorylation of PERK and activation of its downstream signaling (phospho-eIF-2 α) occurred in the presence of palmitate. There was also upregulation of the IRE-1 α -dependent pathway upon treatment with palmitate, illustrated by increased expression of sXBP-1 and its downstream target genes (CHOP and GRP78) (Fig. 5a). Increased phospho-JNK was also observed, which could be directly responsible for the observed insulin resistant state induced by palmitate treatment in Neo cells. Unlike Neo cells, BI-1 cells were relatively resistant to palmitate-induced ER stress. Phosphorylation of PERK in response to palmitate treatment in BI-1 cells was less evident than it was in Neo cells and delayed the expression of phospho-eIF-2 α compared with Neo cells. The IRE-1 α -dependent pathway was comparably less activated by palmitate treatment in BI-1 cells, as shown by the reduced induction of sXBP-1, CHOP, and GRP78 compared with treated Neo cells. Phosphorylation of JNK

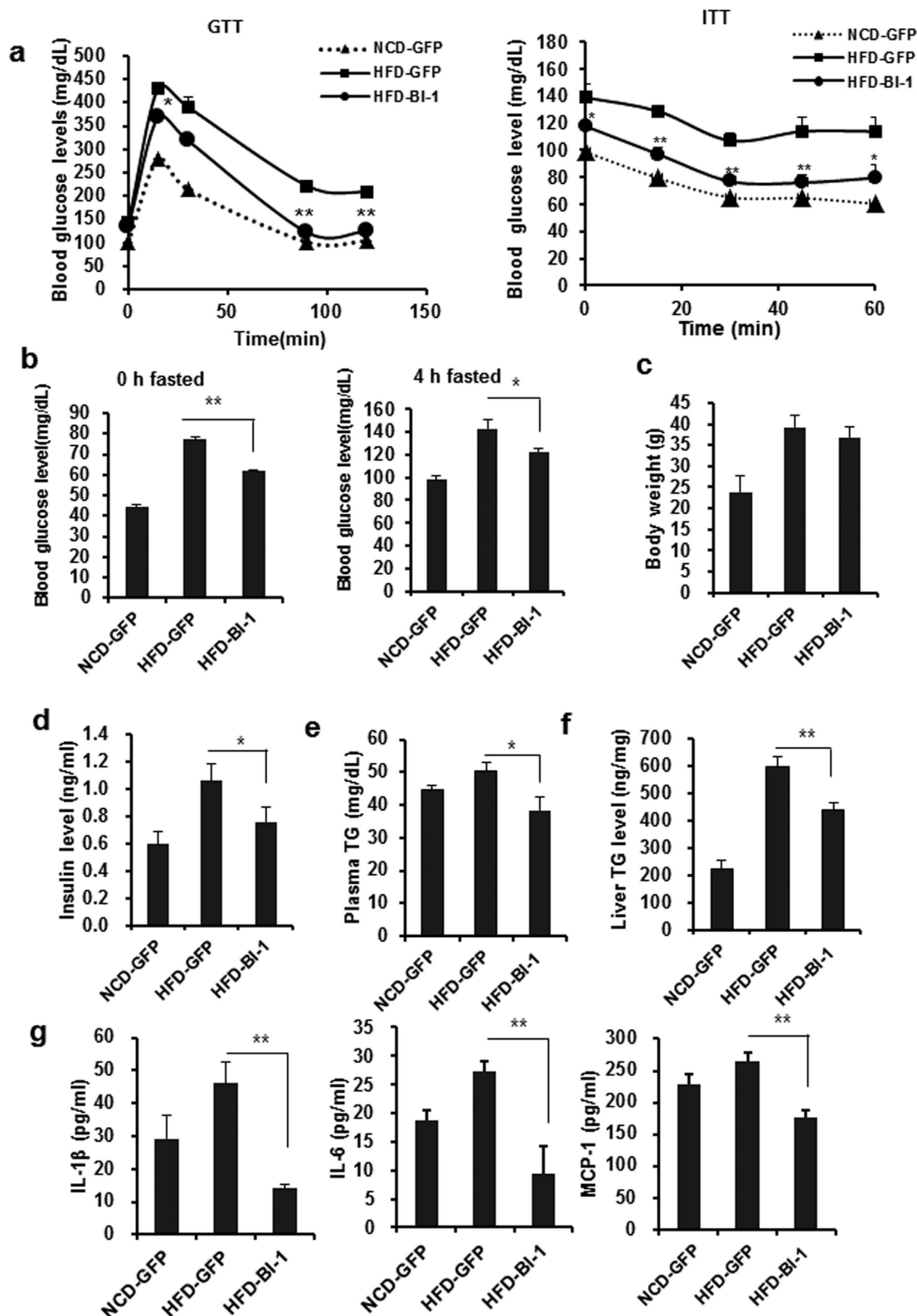


Figure 3. Hepatic BI-1 expression enhances hepatic glucose metabolism and insulin signaling under high-fat diet conditions. (a) Mice were fed normal or high-fat diets. Eight weeks later, GFP or BI-1 adenovirus was injected into mice through tail veins. Four days post-injection, glucose and insulin tolerance tests (GTT and ITT) were performed as described in Materials and Methods ($n = 5-7$ each). (b-g) Fasting glucose (0 h and 4 h) (b), body weight (c), plasma insulin (d), plasma TG (e), liver TG levels (f), and plasma IL-1 β , IL-6, and MCP-1 levels (g) were measured in normal diet-fed mice infected with GFP virus, high-fat diet-fed mice infected with GFP virus, and high-fat diet-fed mice infected with BI-1 adenovirus ($n = 6-10$ each). Data represent mean \pm SEM (* $p < 0.05$, ** $p < 0.01$, t -test).

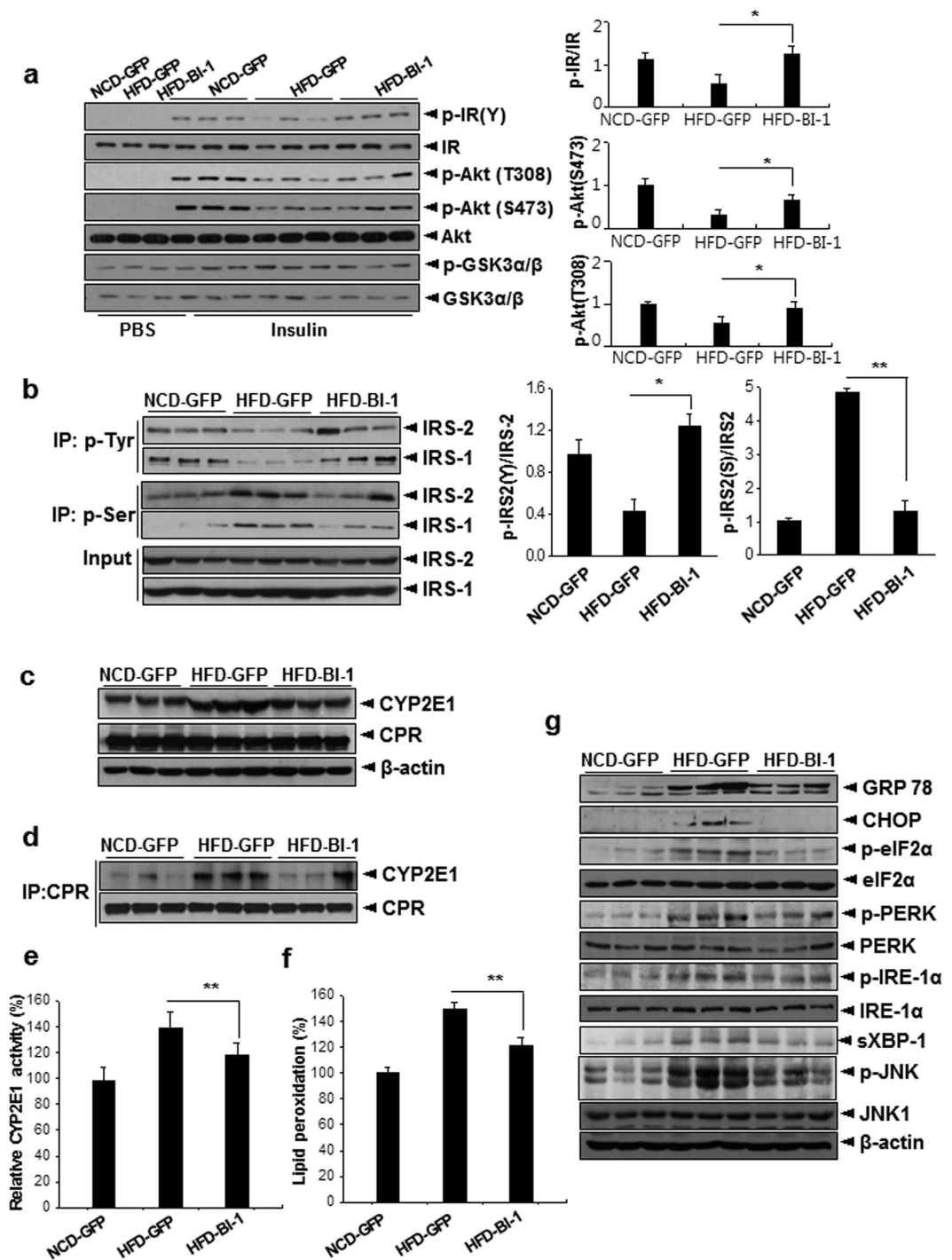


Figure 4. Hepatic BI-1 expression enhances insulin signaling regulation of hepatic CYP2E1 activity, ROS accumulation, and ER stress in high-fat diet-fed mice. (a,b) Western blot analysis showing effects of BI-1 expression on insulin signaling pathway in normal diet-fed or high-fat diet-fed mice injected with GFP adenovirus alone or with GFP plus BI-1 adenovirus. Quantification of p-IR/IR, p-AKT (S473)/AKT, or p-AKT (T308)/AKT was performed (right). Liver lysates were immunoprecipitated with p-Tyrosine or p-Serine antibody and immunoblotted with antibodies against IRS1/2. Quantification of p-Tyr or Ser IRS2/IRS2 was performed (right). (c) Western blot analysis showing effects of BI-1 expression on levels of CYP2E1 and CPR. (d) Co-immunoprecipitation assay of interaction between CPR and CYP2E1 in livers of normal diet-fed or high-fat diet-fed mice injected with GFP adenovirus alone or GFP plus BI-1 adenovirus. Estimation of chlorozoxane hydroxylase activity of CYP2E1 (e) and lipid peroxidation (f) showing ER-stress induced ROS production in livers (each, $n = 5$). (g) Western blot analysis showing effects of BI-1 on ER stress signaling pathways in livers of high-fat diet-fed mice (Representative data performed in three separate measurements, $n = 3-5$). Data represent mean \pm SD ($*p < 0.05$, $**p < 0.01$, t -test).

CPR, CYP2E1, and resulting CYP2E1 activity in Neo cells (Fig. 6a). The induction of ROS by palmitate treatment in BI-1 cells was not as pronounced as in Neo cells (Fig. 6b), indicating that BI-1 also suppresses ROS generation in response to ER stress, perhaps by reducing the activity of CYP2E1 (Fig. 6c). Insulin signaling and ROS generation in response to inhibition of CYP2E1 activity requires confirmation. Treatment with a CYP2E1 inhibitor²³, 4-methylpyrazole, inhibited the ROS accumulation (Fig. 6d) and restored the palmitate-induced regulation of phospho-IRS2 in the presence of insulin in Neo cells (Fig. 6e), suggesting the essential role of CYP2E1 in palmitate-induced insulin resistance in liver cells. Palmitate-induced reduction of phospho-AKT, phospho-FoxO1, and phospho-GSK3 β was also recovered by treatment with 4-methylpyrazole (Fig. 6f). To test the endogenous role of BI-1 at insulin resistance, we applied the same stress, “palmitate at insulin-treated or non-treated condition” in BI-1 knock-out hepatocytes. Expectedly, insulin-dependent increases of tyrosine phosphorylation of both IRS-1 and -2 but there was less prominent in the knock-out cells compared with the control (Fig. 7a). In order to test the impact of CYP2E1 at in the BI-1 knock-out cells, CYP2E1 siRNA was applied to the BI-1 knock-out hepatocytes (Fig. 7b, upper). In the CYP2E1-siRNA-transfected BI-1 knock-out cells, the reduced tyrosine phosphorylation of IRS-1 and -2 was clearly recovered compared with non-specific siRNA-transfected BI-1 knock-out cells. (Figure 7b), and palmitate-induced reduction of phospho-AKT, phospho-FoxO1, and phospho-GSK3 β was also recovered at CYP2E1-siRNA-transfected condition (Fig. 7c). ROS analysis was also performed. Consistently, palmitate-induced ROS production was significantly reduced in the CYP2E1 siRNA-transfected BI-1 knock-out hepatocytes compared with non-specific siRNA-transfected BI-1 knock-out cells (Fig. 7d). These data strongly suggest that CYP2E1 is directly responsible for ROS production and the perturbation of hepatic insulin signaling in response to palmitate-induced ER stress. These data also clarify the role of BI-1 in CYP 2E1 expression and activity.

CYP2E1 enhances palmitate-induced ROS, cell death, and insulin resistance in liver cells. ROS production was higher in HepG2 CYP 2E1 cells than in Neo cells in the basal state, and increases in ROS accumulation in response to palmitate treatment were much more pronounced in CYP2E1 cells than in Neo cells (Fig. 8a). Expression of CYP2E1 enhanced palmitate-induced ER stress and elevated IRE-1-dependent signaling, as shown by enhanced expression of PERK and p-eIF-2 α as well as sXBP-1 and p-JNK, respectively (Fig. 8b). Overexpression of CYP2E1 decreased IRS2 phosphorylation both in the presence and absence of palmitate (Fig. 8c). Phosphorylation of AKT, FoxO1, and GSK3 β was also decreased in CYP2E1 cells compared with Neo cells (Fig. 8d).

Bax-1 inhibits the interconnection between CPR and CYP2E1, leading to insulin sensitivity. Throughout this study, we focus on ROS involvement in insulin resistance. How BI-1 regulates ROS and insulin resistance is a main theme of this study. The binding between NADPH-dependent monoamine oxidase pathway-lined reductase (CPR) and BI-1, which decreases the interaction between CPR and CYP2E1, is thought to be a mechanism of ROS and related insulin resistance regulation by BI-1. Figure 9 clearly explains the main scheme of BI-1-induced regulation of insulin resistance. However, recent evidence shows that BI-1 is an inhibitor of the IRE1 α branch of the UPR, and interferes with IRE1 α endonuclease activity²⁴. Therefore, we compared the binding status of BI-1 with CPR and IRE-1 α . In the absence of treatment, the association of BI-1 with CPR and with IRE-1 α was confirmed (Fig. S11). Under free fatty acid stress, the interaction of BI-1 with IRE-1 α was less stable compared with that of BI-1 with CPR. Although binding intensity might be not a critical parameter explaining biological function, the stable association of BI-1 with CPR is suggested to be a regulatory mechanism of BI-1 against ROS and insulin resistance.

Discussion

Our previous studies suggested that BI-1 is an ER stress regulator that also inhibits the activity of CYP2E1. This study identified CYP2E1 as a crucial player in ER stress-induced ROS production, supporting our hypothesis that the antagonistic activity of BI-1 against ER stress-induced insulin resistance in liver cells is due to inhibition of ROS via interconnection between CPR and CYP2E1. The BI-1 knock-out mouse results also showed that BI-1 can function to inhibit ER stress-induced insulin resistance.

Electron uncoupling between CYP2E1 and CPR has been considered a source of ROS⁸ potentially linked to the dysregulation of insulin resistance in hepatocytes²⁵. In addition, increased infusion of saturated fat into the liver may be critical in promoting insulin resistance in this organ^{26,27}. Insulin resistance leads to a spectrum of non-alcoholic fatty liver diseases, with manifestations ranging from pure steatosis to non-alcoholic steatohepatitis, which can evolve to cirrhosis^{27,28}. In the presence of infused saturated fat, liver cells are continuously subject to insults from ROS (reactive oxygen species). These include free radicals such as the superoxide radical (O₂⁻) and H₂O₂, a common feature of non-alcoholic fatty liver diseases.

BI-1, an ER stress regulator, increased insulin sensitivity via regulation of IRS-2 (p-Tyr and p-Ser) phosphorylation in free fatty acid-exposed liver cells (Fig. 5c). Non-alcoholic fatty liver diseases patients have increased lipolysis and increased delivery of free fatty acids to the liver. Higher free fatty acid concentrations are associated with more severe liver disease^{29,30}. In *in vitro* approaches, palmitate has been used to study the effect of free fatty acids on hepatic signaling by mimicking conditions of hepatic diseases such as non-alcoholic fatty liver diseases. ER stress and JNK activation have been suggested as major instigators of insulin resistance, a main component of the non-alcoholic fatty liver diseases-associated phenomena^{31–34}. Palmitate and high-fat diet conditions were found to stimulate IRE-1 α and PERK signaling transduction (Figs 2e,4g and 5a), among other ER stress proteins. Similarly, the two arms of ER stress signaling mentioned above have been suggested to be main mechanisms of lipid metabolism disturbance and insulin sensitivity dysregulation^{35–37}. In contrast to the results of multiple ER stress-involvement studies, in mice placed on a 3-day high fat diet, one specific ER stress arm, eIF2 α signaling, exhibited high levels of induced hepatic lipid accumulation and insulin resistance³⁰. Recently, apoB100 protein

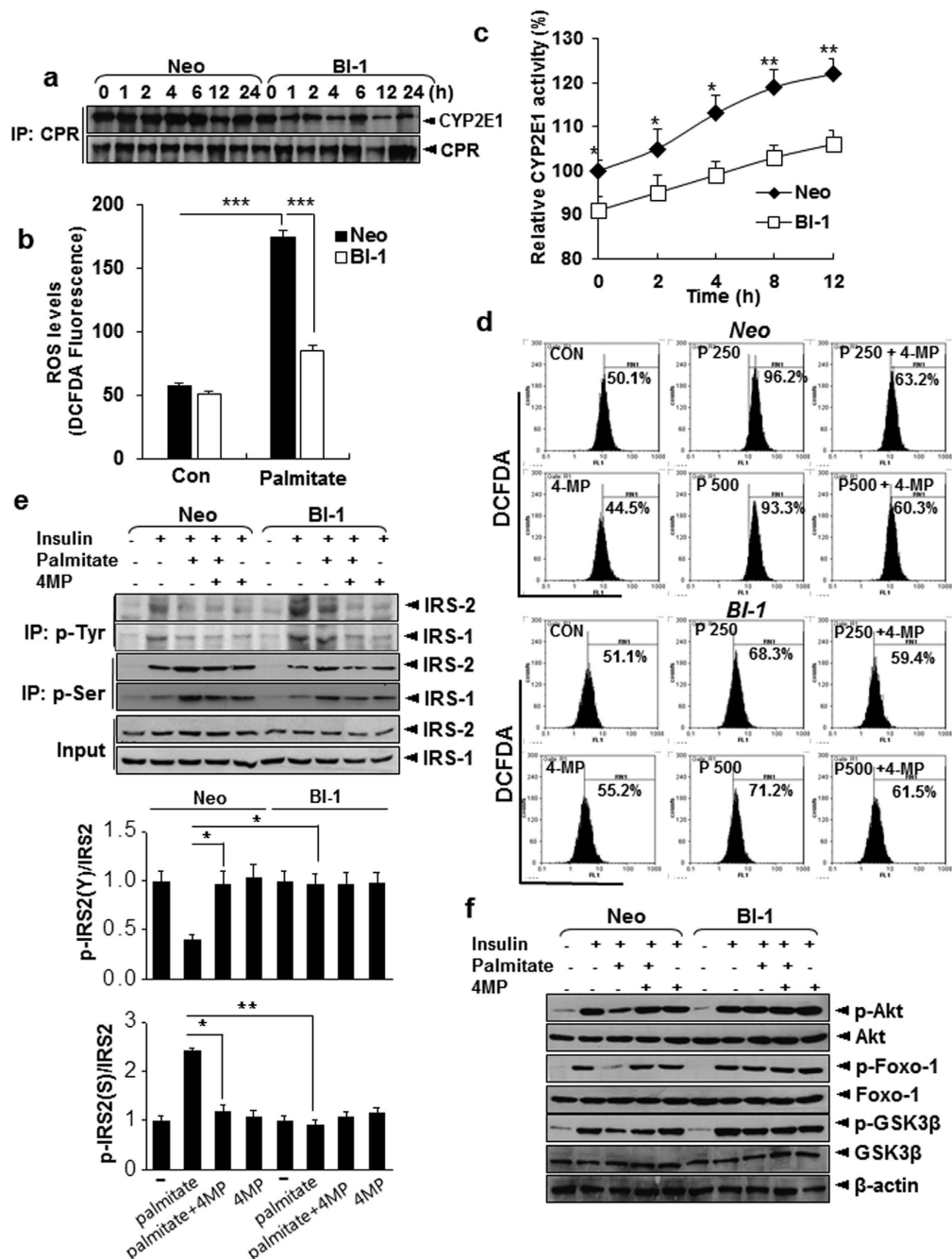


Figure 6. Effects of BI-1 on hepatic ROS production and insulin signaling are mediated by CYP2E1 regulation. (a) Co-immunoprecipitation assay demonstrating effects of BI-1 on palmitate-induced interaction of CYP2E1 with CPR. Neo and BI-1 cells were treated with 250 μ M palmitate for indicated periods. (b) DCF-DA assay revealing palmitate-induced ROS production in Neo and BI-1 cells. Neo and BI-1 cells were treated with 250 μ M palmitate for 12 h. DCF-DA, 100 μ M, was loaded into cells and fluorescence was measured. (c) Chlorozoxane hydroxylation activity assay showing effects of BI-1 expression on CYP2E1 activity. Hepatic microsomes were treated with chlorozoxane (500 nmol) in a total volume of 1 ml. (d) DCF-DA assay showing palmitate-induced ROS production in Neo and BI-1 cells in the presence or absence of 1 mM 4-MP. Palmitate, 250 or 500 μ M, was administered to cells for 12 h, then 100 μ M DCF-DA was loaded for 30 min. After washing, fluorescence was measured by FACS analysis. (e,f) Neo and BI-1 cells were treated with or without 1 mM 4-MP, an inhibitor of CYP2E1, in the presence or absence of 250 μ M palmitate and/or 100 nM insulin. Western blot analysis showing effects of 4-MP on palmitate-mediated reduction in tyrosine or serine phosphorylation of IRS1 and IRS2 in Neo and BI-1 cells. Cell lysates were immunoprecipitated with p-tyrosine or p-serine 307 antibody and immunoblotted with anti-IRS1 and anti-IRS2 antibodies (e). Quantitation of phospho-Tyr and phospho-Ser IRS2. Data represent mean \pm SEM. Western blot analysis demonstrating effects of 4-MP on downstream insulin signaling pathway (f). Data in (b,c,e) ($n = 6$) represent mean \pm SD (* $p < 0.05$, ** $p < 0.005$, *** $p < 0.0005$, t -test). (a,d) and (f) Representative data performed in three separate measurements.

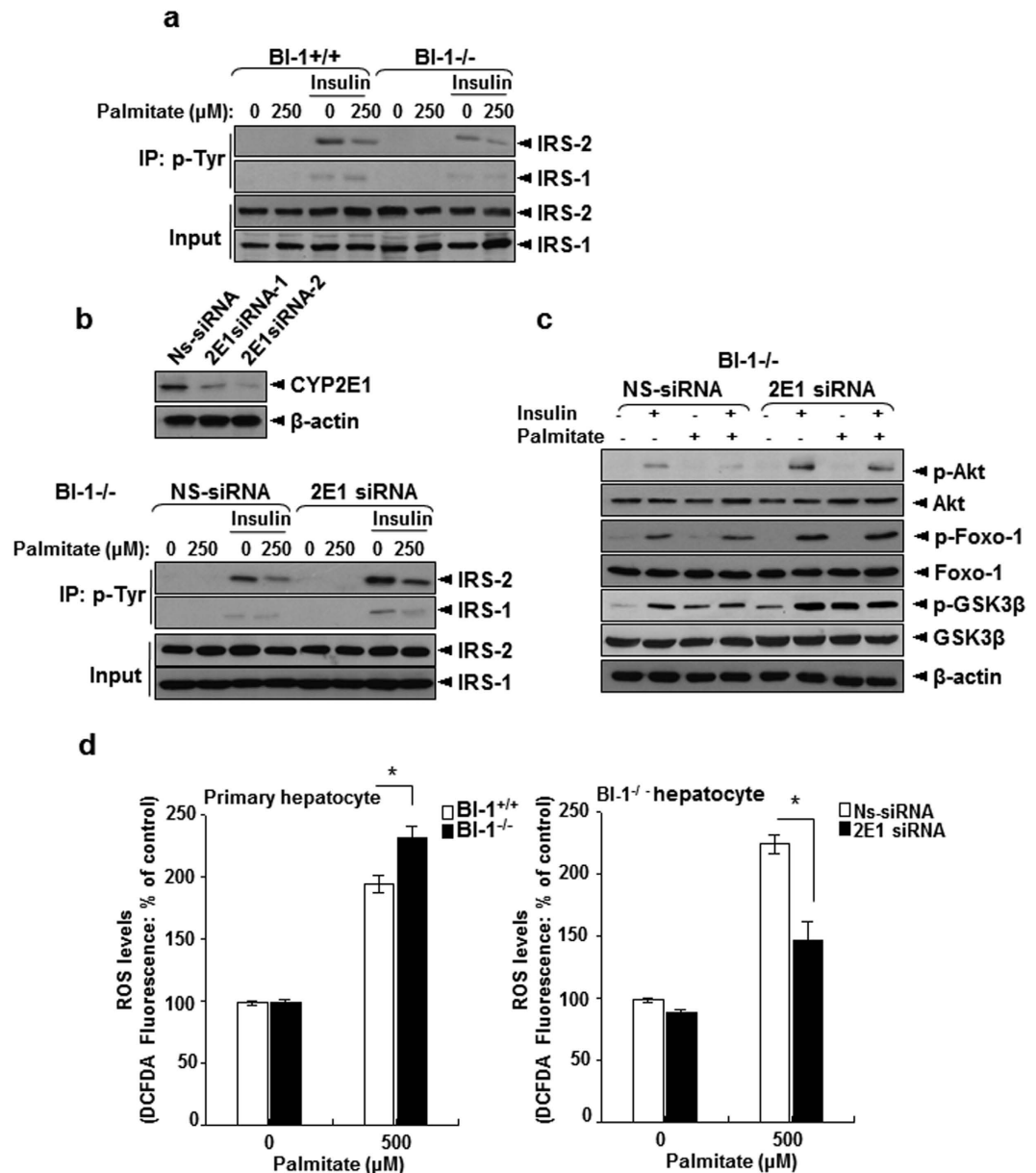


Figure 7. CYP2E1 induces insulin resistance and ROS production in BI-1 knock-out primary hepatocytes.

Primary hepatocytes from BI-1 wild-type and BI-1 knock-out mice were treated with 250 μM palmitate in presence or absence of insulin. Cell lysates were immunoprecipitated with p-Tyrosine antibody and immunoblotted with antibodies against IRS1/2 (a). Hepatocytes from BI-1 knock-out mice were transiently transfected with non-specific-siRNA or CYP2E1 siRNA. Cells were treated with 250 μM palmitate in presence or absence of insulin. Cell lysates were immunoprecipitated with p-Tyrosine antibody and immunoblotted with antibodies against IRS1/2 (b). The Cell lysates were immunoblotted with anti-p-Akt, Akt, p-FoxO1, FoxO1, p-GSK3β, GSK3β or β-actin antibody (c). In non-specific-siRNA or CYP2E1 siRNA-transfected BI-1 knock-out hepatocytes, 250 μM palmitate was treated for 12 h, then 100 μM DCF-DA was loaded for 30 min. After washing, fluorescence was measured by FACS analysis (d). Representative data performed in three separate measurements.

synthesis was studied in relation to one branch of the ER stress pathways, PERK activation³⁸. Bailly-Maitre B *et al.* demonstrated that HFD induces only a single arm of ER stress, IRE-1α, and its related insulin resistance²⁹, and inhibition of this arm by BI-1 expression has been suggested previously, in contrast to the results of this study. The interaction of BI-1 with IRE-1α^{24,39} is considered a mechanism against insulin resistance. Our study also included the association between IRE-1α and BI-1 (Fig. S11). Considering that the interaction between BI-1 and IRE-1α was diminished after relatively long time periods (more than 6 hours of treatment), the interaction of IRE-1α with BI-1 may not be stable under free fatty acid stress, in contrast to the stable interaction between CPR and BI-1. The regulation effect of BI-1 on insulin resistance signaling was clearly shown at the 12-hour time point (Figs 5c and 6e), when a slight binding affinity with IRE1α was observed. Possible competition between CPR and IRE-1α

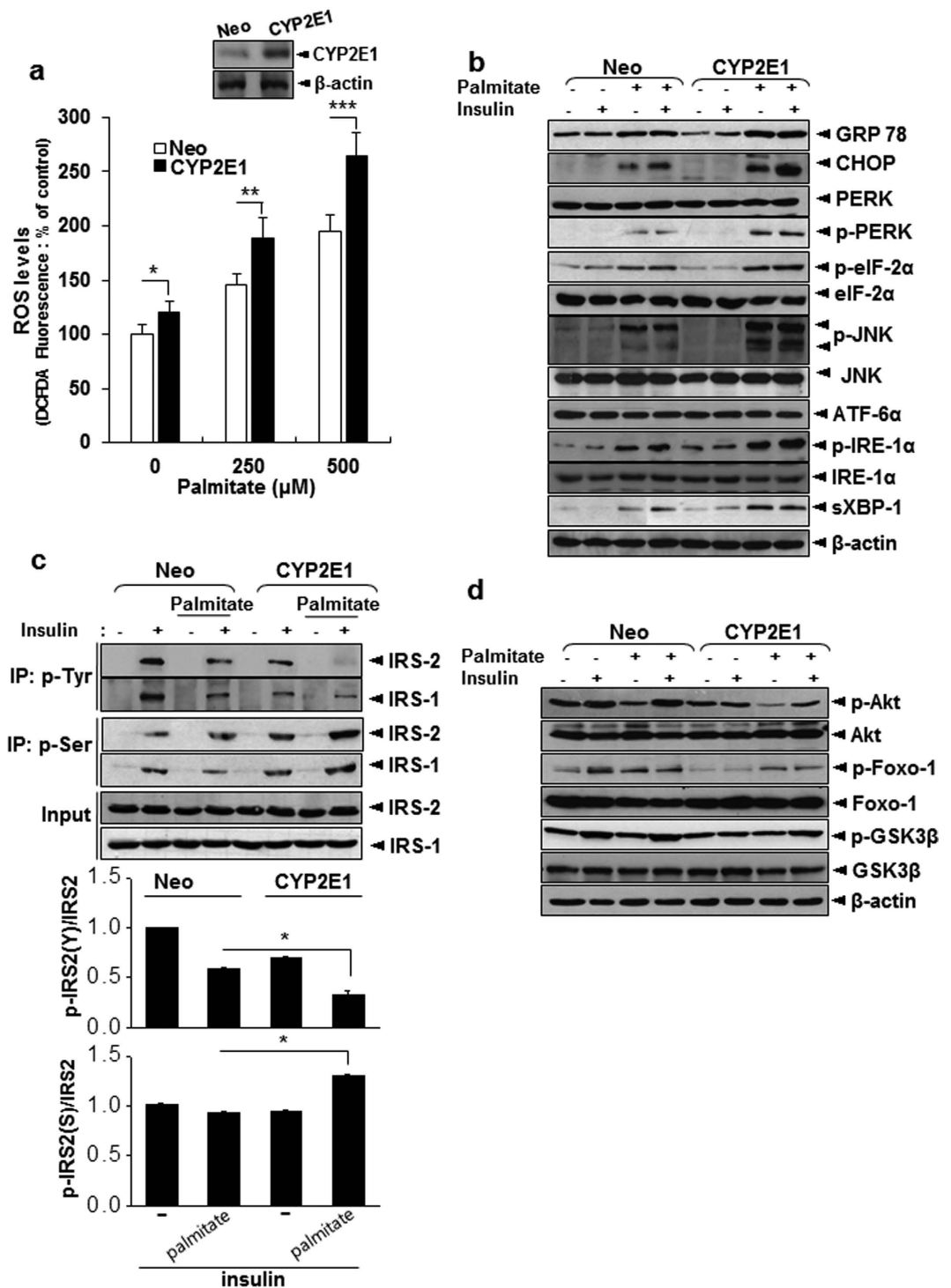


Figure 8. CYP2E1 promotes palmitate-induced ER stress and insulin resistance. (a) DCF-DA assay showing palmitate-induced ROS production in Neo and CYP2E1 cells. (b) Western blot analysis demonstrating effects of CYP2E1 expression on palmitate-induced ER stress response. (c,d) Neo and CYP2E1 cells were treated with 250 μM palmitate in presence or absence of 100 nM insulin. Western blot analysis showing effects of CYP2E1 on tyrosine and serine 307 phosphorylation of IRS1 and IRS2, and quantification of tyrosine and serine 307 phosphorylation of IRS2 (c) and its downstream proteins (d). Data in (a,c) ($n = 4$) represent mean \pm SD (* $p < 0.05$, ** $p < 0.005$, *** $p < 0.0005$, t -test). (b,d), Representative data performed in three separate measurements.

for association with BI-1 should be considered. This study suggests that the stable binding of BI-1 with CPR is another regulatory mechanism of insulin resistance, in addition to IRE1- α . BI-1 binds to CPR to dissociate it

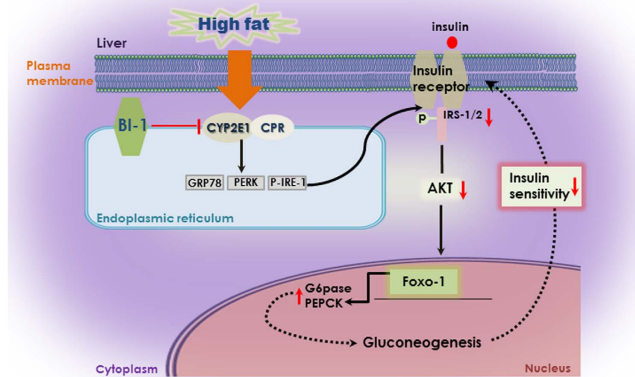


Figure 9. Schematic mechanism of protective role of BI-1 against insulin resistance.

from CYP2E1 and subsequently inhibit ROS production, suggesting that BI-1-mediated inhibition of CYP2E1 activity may decrease ROS production and ER stress. CYP2E1 knock-out mice displayed consistent, substantial protection against high fat diet-induced hepatic insulin resistance and insulin-stimulated adipose tissue glucose uptake, providing evidence that CYP2E1 is a negative regulator of glucose and energy metabolism^{40–42}. Increased oxidative stress has been implicated as a causative factor in insulin resistance, and considerable increases in oxidative stress markers in diabetes and related conditions have also been reported⁴³. Mitochondria-associated ROS are involved in the dysregulation of lipid metabolism and insulin resistance^{44,45}, although no impairments in mitochondrial function have been observed with the activation of the two major ER stress pathways (PERK/eIF2 α and IRE1/XBP1) in a non-alcoholic fatty liver disease model⁴⁶. Recently, the amplified ROS connection between mitochondria and ER has also attracted attention in this field^{47,48}, indicating that the subcellular organelle-connected transfer/communication of ROS signaling might be interrelated, ultimately leading to biological changes including cellular dysmetabolism and insulin resistance^{49,50}. Interestingly, a significant amount of CYP2E1 has been suggested to be localized within liver mitochondria, inducing mitochondrial dysfunction and insulin resistance and also suggesting the possibility of connected ROS signaling between the ER and mitochondria through CYP2E1¹². Through CYP2E1, intra-ER oxidative stress has been also reported, suggesting that ER protein-folding machinery capacitance might be affected, leading to ER stress and related physio/pathological changes, particularly hepatic lipid dysmetabolism⁵¹.

CYP2E1 induction of oxidative stress impairs insulin signaling to IRS-1, IRS-2, PI3-kinase, and Akt/PKB^{42,52–55} and the CYP2E1-mediated oxidative stress is one of the key mechanisms for ER dysfunction⁵⁶. The CYP2E1 is directly or indirectly linked to intra-ER altered protein folding, where ROS accumulation is suggested to alter ER folding^{57,58}. CPR, ER-localized NADPH-dependent oxygenase (NOX4)⁵⁹ and other NADPH-linked oxidative folding machinery such as protein disulfide isomerase (PDI) and endoplasmic reticulum oxidoreductase (ERO)⁶⁰ are possible candidate proteins for intra-ER-originating ROS-linked protein folding alterations, which lead to ER stress and hepatic dyslipidemic insulin resistance. In our model, a high fat diet might induce conditions similar to xenobiotic treatment conditions in which CYP machinery is involved. The main factor for the mentioned proteins-associated ER-redox coupling/uncoupling seems to be NADPH. With intra-ER coupling of NADPH, the PDI/ERO1 α -oxidoreduction process also amplifies CYP initiation of ROS production, which induces protein aggregation and the ER stress response⁸. Another basic characteristic of BI-1, the Ca²⁺ leaky channel effect, may be considered a potential mechanism involved in palmitate-induced ROS and insulin resistance. ER calcium release and resultant mitochondrial dysfunction have been suggested as a mechanism involved in palmitate-induced ROS²². It has been also suggested that insulin resistance depends on intracellular Ca²⁺ and ROS^{10,61}.

In summary, we showed that BI-1 overexpression protects hepatocytes from ROS accumulation and insulin resistance in response to palmitate-induced ER stress conditions. Knock-out of BI-1 in mice exacerbates glucose intolerance and impairs insulin signaling induced by high-fat diet-induced chronic ER stress. The regulatory role of BI-1 is mediated by inhibition of CYP2E1 expression and interaction between CPR and CYP2E1. These data suggest that BI-1 may serve as a novel therapeutic target protein for the treatment of ER stress-induced hepatic insulin resistance.

Materials and Methods

Materials. Palmitate was purchased from Calbiochem (San Diego, CA, USA). DCF-DA (2',7'-dichlorofluorescein diacetate) was obtained from Molecular Probes (Eugene, OR, USA). Antibodies against β -actin, GRP78, CHOP, ATF6 α , p-PERK, sXBP-1, p-JNK, Akt, Foxo1, GSK3 β , IRS-1, IRS-2, HSP90, and CPR were acquired from Santa Cruz Biotechnology (Santa Cruz, CA, USA). Antibodies against p-AKT, p-Foxo-1,

Foxo-1, p-AKT, p-GSK3 β , p-Tyr, p-IR, and IR were acquired from Cell Signaling Technology (Beverly, MA, USA). Chlorozoxazone and p-nitrophenol were purchased from Sigma-Aldrich Co. (St. Louis, MO, USA).

Animal experiments. BI-1 wild type (BI-1^{+/+}) and BI-1 knock-out (BI-1^{-/-}) mice were obtained from Dr. John C. Reed at the Stanford-Burnham Institute for Medical Research (La Jolla, CA, USA). All animal experiments were carried out in accordance with the National Research Council's Guidelines (IACUC, Knock-outrea) for the Care and Use of Laboratory Animals. The experimental protocol was approved by the Animal Experiments Committee of Chonbuk National University Laboratory Animal Center (CBU 2013-0015).

Animals were housed in standard 75-in2 static cages. The cages and bedding were autoclaved prior to use. All husbandry practices aside from housing density were in accordance with the Knock-outrea Association for Laboratory Animal Science Guide. Cages were changed once or twice per week, depending on need. To induce obesity and insulin resistance, 8-week-old male C57BL/6, BI-1 wide-type and BI-1 knock-out mice were fed a high-fat diet (60 kcal% fat diet: D12492 of Research Diets) for 8 weeks. Animal experiments involving adenoviruses were performed as described previously⁶². To measure fasting blood glucose level, animals were fasted for 16 h or 6 h with free access to water. For glucose tolerance test (GTT), 16 h-fasted mice were injected intraperitoneally with glucose (1.5 g/kg of body weight for high-fat diet). For insulin tolerance test (ITT), 6 h-fasted mice were injected intraperitoneally with 0.5 unit/kg (high-fat diet) body weight of insulin. Blood glucose levels were measured from tail vein blood collected at the designated time.

Recombinant adenoviruses. Adenoviruses expressing GFP only and BI-1 were generated by homologous recombination between adenovirus backbone vector pAD-Easy and linearized transfer vector pADTrack. For animal experiments, viruses were purified on a CsCl gradient, dialyzed against PBS buffer containing 10% glycerol, and stored at -80 °C.

Histology. Histology works were performed on frozen liver sections from BI-1 wide-type ($n = 6$) and BI-1 knock-out ($n = 6$) mice. Hematoxylin and eosin (H&E) stains showed nuclei and cytoplasm in liver tissue. Oil-red O staining on these frozen liver sections were performed for detecting lipid droplets.

Quantitative PCR. Total RNA from liver tissue was extracted using Easy-spin total RNA extract kit (Qiagen). 1 mg of total RNA was used for generating cDNA with amfiRivert reverse transcriptase (GenDEPOT), and was analyzed by quantitative PCR using SYBR green PCR kit and Bio-Rad Real Time System. All data were normalized to expression of ribosomal L32.

Measurement of metabolites. Blood glucose levels were determined from tail vein blood using an automatic glucose monitor (One Touch; LifeScan, Inc.). Plasma triglyceride and non-essential fatty acid were measured accordingly with the protocols of the colorimetric assay kits (Waknock-out). Plasma insulin was measured accordingly with the protocols of the Mouse Insulin ELISA Kit (ALPCO). Total liver lipids were extracted with chloroform-methanol (2:1, v/v) mixture as described previously²⁶.

Generation of Neo and BI-1 stable cell lines. HA-pcDNA3-BI-1 and Neo-pcDNA3 plasmids (Neo: containing neomycin-selection marker) were stably transfected into 80% confluent HepG2 cells with lipofectamine (Invitrogen, CA). G418 (1 mg/mL; Waknock-out) was used for selection. Neo and BI-1 stably transfected HepG2 cell lines were generated and used during this study.

DCF-DA assay. Intracellular ROS levels were measured as previously described²⁷. After treatment of palmitate with or without 4-MP or palmitate with or without insulin, the cells were incubated with 100 μ M 2',7'-dichlorofluorescein diacetate (DCF-DA) at 37 °C for 30 min. The fluorescence intensity of 2',7'-dichlorofluorescein formed by a reaction between DCF-DA and intracellular ROS was analyzed by PAS flow cytometry (Partec, Münster, Germany) at excitation and emission wavelengths of 488 and 525 nm, respectively. Data are expressed as representative histograms from three independent experiments.

Microsomal fractionation. The microsomal fraction was obtained as previously described⁸. Briefly, the cells were re-suspended in buffer A (250 mM sucrose, 20 mM HEPES, pH 7.5, 10 mM KCl, 1.5 mM MgCl₂, 1 mM EDTA, 1 mM EGTA, and 1 \times protease inhibitor complex (Roche Diagnostics, Mannheim, Germany) on ice for 30 min. The cells were homogenized and the lysates centrifuged at 750 g for 10 min at 4 °C to remove the non-lysed cells and nuclei. The supernatant was then centrifuged at 100,000 g for 1 h at 4 °C. The resulting supernatant was discarded, and the pellet was saved as the light membrane (LM:ER/microsome) fraction.

Western blotting. For Western blotting, whole-cell lysates were generated by using a buffer consisting of 1% Nonidet P-40, 50 mM HEPES (pH 7.5), 100 mM NaCl, 2 mM EDTA, 1 mM pyrophosphate, 10 mM sodium orthovanadate, 1 mM phenylmethylsulfonyl fluoride, and 100 mM sodium fluoride. Equal amounts of lysates were subjected to sodium dodecyl sulfate-10% polyacrylamide gel electrophoresis and then transferred to Immobilon-P membranes (Millipore) in transfer buffer (25 mM Tris, 192 mM glycine, 20% [vol/vol] methanol). Membranes were first rinsed in Tris-buffered saline (TBS: 10 mM Tris [pH 7.4], 150 mM NaCl) and then blocked overnight at room temperature in TBS-5% bovine serum albumin (BSA). Various antibodies were used at a dilution of 1:1000 in TBS-5% BSA. Antibody-antigen complexes were detected with horseradish peroxidase-conjugated protein A or horseradish peroxidase-conjugated goat anti-rabbit immunoglobulin G (Bio-Rad) and a chemiluminescent substrate development kit (Amersham, CA, USA). Equal loading was ascertained by the presence of β -actin.

Immunoprecipitation. Immunoprecipitation was performed as previously described¹. For immunoprecipitation, cell lysates were prepared in 50 mM Tris-HCl, pH 8.0, containing 150 mM NaCl, 0.015%

phenylmethylsulfonyl fluoride, 1 mM dithiothreitol, 1 mM EDTA, 1% sodium deoxycholate, 1% Triton, and 1% SDS. Cell lysates were incubated at 70 °C for 15 min to ensure complete cell lysis and diluted with lysis buffer to achieve SDS concentration of 0.1% (w/v), as reported. Media were collected and centrifuged at 13,000 rpm for 10 min to remove cell debris. Supernatants (0.9 ml) were combined with 0.1 ml of 10 X lysis buffer containing 1% SDS. Cell lysates and media were incubated with antibodies (1:100 dilution) for 2 h and then with 20 µl of protein A/G-Sepharose (10% solution) for an additional 2 h. Immuno-complexes were collected by centrifugation, washed three times with 10 mM Tris, pH 7.5, containing 0.1 M NaCl and 1% Triton, eluted in 50 µl of sample buffer, separated on SDS-polyacrylamide gel, and Western blotting were performed as described in the section of Western blotting.

CYP 2E1 siRNA transfection. Primary mouse hepatocytes were isolated from BI-1 wide-type and BI-1 knock-out by collagenase digestion, following a previously described protocol⁶³. Scramble, CYP2E1-1, and CYP 2E1-2 siRNAs were purchased from Bioneer (Bioneer, Daejeon, Korea). The scramble-sense siRNA targeted the sequence 5'-CCUACGCCACCAAUUUCGU-3', and the scramble-antisense siRNA targeted the sequence 5'-CGAAAUUGGUGGCGUAGG-3'. CYP 2E1-1-sense siRNA targeted the sequence 5'-GAUUACGAUGACAAGAAGU (dTdT)-3', and CYP 2E1-1-antisense siRNA targeted the sequence 5'-ACUUCUUGUCAUCGUAAUC (dTdT)-3'. CYP 2E1-2-siRNA targeted the sequence 5'-UCAACCUCGUCCCUCCAA (dTdT)-3', and CYP 2E1-2-siRNA -antisense siRNA targeted the sequence 5'-UUGGAAGGACGAGGUUGA (dTdT)-3'. For transient transfection, cells were plated to obtain 70–80% confluence in 10-cm dish. After overnight incubation, plated primary hepatocytes were transfected with 50 nM of scramble (negative control) siRNA, CYP 2E1-1, or CYP 2E1-2 using Lipofectamine[®] 3000 (Invitrogen, Carlsbad, CA, USA). After 24 h of transfection, fresh medium was exchanged.

Statistical Analysis. Statistical differences were evaluated by analysis of variance (ANOVA) in acidity level-response experiments and two-tailed Student's *t*-tests. In each case, the statistical test used is indicated, and the number of experiments is stated individually in the legend of each figure.

References

- Xu, Q. & Reed, J. C. Bax inhibitor-1, a mammalian apoptosis suppressor identified by functional screening in yeast. *Molecular cell* **1**, 337–346 (1998).
- Lee, G. H. *et al.* Bax inhibitor-1 regulates endoplasmic reticulum stress-associated reactive oxygen species and heme oxygenase-1 expression. *The Journal of biological chemistry* **282**, 21618–21628, doi: 10.1074/jbc.M700053200 (2007).
- Chae, H. J. *et al.* BI-1 regulates an apoptosis pathway linked to endoplasmic reticulum stress. *Molecular cell* **15**, 355–366, doi: 10.1016/j.molcel.2004.06.038 (2004).
- Lee, G. H., Kim, H. R. & Chae, H. J. Bax inhibitor-1 regulates the expression of P450 2E1 through enhanced lysosome activity. *The international journal of biochemistry & cell biology* **44**, 600–611, doi: 10.1016/j.biocel.2011.12.017 (2012).
- Premereur, N., Van den Branden, C. & Roels, F. Cytochrome P-450-dependent H₂O₂ production demonstrated *in vivo*. Influence of phenobarbital and allylisopropylacetamide. *FEBS letters* **199**, 19–22 (1986).
- Davydov, D. R. Microsomal monoxygenase in apoptosis: another target for cytochrome c signaling? *Trends in biochemical sciences* **26**, 155–160 (2001).
- Nieto, N., Friedman, S. L. & Cederbaum, A. I. Stimulation and proliferation of primary rat hepatic stellate cells by cytochrome P450 2E1-derived reactive oxygen species. *Hepatology* **35**, 62–73, doi: 10.1053/jhep.2002.30362 (2002).
- Kim, H. R. *et al.* Bax inhibitor 1 regulates ER-stress-induced ROS accumulation through the regulation of cytochrome P450 2E1. *Journal of cell science* **122**, 1126–1133, doi: 10.1242/jcs.038430 (2009).
- Zhou, Q. G., Zhou, M., Lou, A. J., Xie, D. & Hou, F. F. Advanced oxidation protein products induce inflammatory response and insulin resistance in cultured adipocytes via induction of endoplasmic reticulum stress. *Cellular physiology and biochemistry: international journal of experimental cellular physiology, biochemistry, and pharmacology* **26**, 775–786, doi: 10.1159/000322345 (2010).
- Kennedy, A. *et al.* Inflammation and insulin resistance induced by trans-10, cis-12 conjugated linoleic acid depend on intracellular calcium levels in primary cultures of human adipocytes. *Journal of lipid research* **51**, 1906–1917, doi: 10.1194/jlr.M005447 (2010).
- Ge, X., Liu, Z., Qi, W., Shi, X. & Zhai, Q. Chromium (VI) induces insulin resistance in 3T3-L1 adipocytes through elevated reactive oxygen species generation. *Free radical research* **42**, 554–563, doi: 10.1080/10715760802155113 (2008).
- Aubert, J., Begrich, K., Knockaert, L., Robin, M. A. & Fromenty, B. Increased expression of cytochrome P450 2E1 in nonalcoholic fatty liver disease: mechanisms and pathophysiological role. *Clinics and research in hepatology and gastroenterology* **35**, 630–637, doi: 10.1016/j.clinre.2011.04.015 (2011).
- Zisner, D. K. Fewer, but tighter, payer relationships expected to underpin integrated health system strategies in the future. *Journal of healthcare management/American College of Healthcare Executives* **58**, 395–398 (2013).
- Bloch-Damti, A. *et al.* Differential effects of IRS1 phosphorylated on Ser307 or Ser632 in the induction of insulin resistance by oxidative stress. *Diabetologia* **49**, 2463–2473, doi: 10.1007/s00125-006-0349-6 (2006).
- Guo, H. *et al.* Cyanidin 3-glucoside protects 3T3-L1 adipocytes against H₂O₂ or TNF- α -induced insulin resistance by inhibiting c-Jun NH2-terminal kinase activation. *Biochemical pharmacology* **75**, 1393–1401, doi: 10.1016/j.bcp.2007.11.016 (2008).
- Jensen, C. B. *et al.* Altered PI3-kinase/Akt signalling in skeletal muscle of young men with low birth weight. *PloS one* **3**, e3738, doi: 10.1371/journal.pone.0003738 (2008).
- Newsholme, P. *et al.* Diabetes associated cell stress and dysfunction: role of mitochondrial and non-mitochondrial ROS production and activity. *The Journal of physiology* **583**, 9–24, doi: 10.1113/jphysiol.2007.135871 (2007).
- Guichard, C., Moreau, R., Pessayre, D., Epperson, T. K. & Krause, K. H. NOX family NADPH oxidases in liver and in pancreatic islets: a role in the metabolic syndrome and diabetes? *Biochemical Society transactions* **36**, 920–929, doi: 10.1042/BST0360920 (2008).
- Gao, D. *et al.* The effects of palmitate on hepatic insulin resistance are mediated by NADPH Oxidase 3-derived reactive oxygen species through JNK and p38MAPK pathways. *The Journal of biological chemistry* **285**, 29965–29973, doi: 10.1074/jbc.M110.128694 (2010).
- Brown, M. S. & Goldstein, J. L. Selective versus total insulin resistance: a pathogenic paradox. *Cell Metab* **7**, 95–96, doi: S1550-4131(07)00382-8 [pii]10.1016/j.cmet.2007.12.009 (2008).
- Yin, J. *et al.* *In vivo* anti-osteoporotic activity of isotaxiresinol, a lignan from wood of *Taxus yunnanensis*. *Phytomedicine: international journal of phytotherapy and phytopharmacology* **13**, 37–42, doi: 10.1016/j.phymed.2004.06.017 (2006).

22. Egnatchik, R. A., Leamy, A. K., Jacobson, D. A., Shiota, M. & Young, J. D. ER calcium release promotes mitochondrial dysfunction and hepatic cell lipotoxicity in response to palmitate overload. *Molecular metabolism* **3**, 544–553, doi: 10.1016/j.molmet.2014.05.004 (2014).
23. Collom, S. L. *et al.* CYP2E1 substrate inhibition. Mechanistic interpretation through an effector site for monocyclic compounds. *The Journal of biological chemistry* **283**, 3487–3496, doi: 10.1074/jbc.M707630200 (2008).
24. Sano, R. *et al.* Endoplasmic reticulum protein BI-1 regulates Ca(2)(+)-mediated bioenergetics to promote autophagy. *Genes & development* **26**, 1041–1054, doi: 10.1101/gad.184325.111 (2012).
25. Leung, T. M. & Nieto, N. CYP2E1 and oxidant stress in alcoholic and non-alcoholic fatty liver disease. *Journal of hepatology* **58**, 395–398, doi: 10.1016/j.jhep.2012.08.018 (2013).
26. Nagle, C. A. *et al.* Hepatic overexpression of glycerol-sn-3-phosphate acyltransferase 1 in rats causes insulin resistance. *The Journal of biological chemistry* **282**, 14807–14815, doi: 10.1074/jbc.M611550200 (2007).
27. Pessayre, D. & Fromenty, B. NASH: a mitochondrial disease. *Journal of hepatology* **42**, 928–940, doi: 10.1016/j.jhep.2005.03.004 (2005).
28. Fromenty, B., Robin, M. A., Igoudjil, A., Mansouri, A. & Pessayre, D. The ins and outs of mitochondrial dysfunction in NASH. *Diabetes & metabolism* **30**, 121–138 (2004).
29. Bailly-Maitre, B. *et al.* Hepatic Bax inhibitor-1 inhibits IRE1alpha and protects from obesity-associated insulin resistance and glucose intolerance. *The Journal of biological chemistry* **285**, 6198–6207, doi: 10.1074/jbc.M109.056648 (2010).
30. Birkenfeld, A. L. *et al.* Influence of the hepatic eukaryotic initiation factor 2alpha (eIF2alpha) endoplasmic reticulum (ER) stress response pathway on insulin-mediated ER stress and hepatic and peripheral glucose metabolism. *The Journal of biological chemistry* **286**, 36163–36170, doi: 10.1074/jbc.M111.228817 (2011).
31. Malhi, H., Bronk, S. F., Werneburg, N. W. & Gores, G. J. Free fatty acids induce JNK-dependent hepatocyte lipopoptosis. *The Journal of biological chemistry* **281**, 12093–12101, doi: 10.1074/jbc.M510660200 (2006).
32. Borradaile, N. M. *et al.* A critical role for eukaryotic elongation factor 1A-1 in lipotoxic cell death. *Molecular biology of the cell* **17**, 770–778, doi: 10.1091/mbc.E05-08-0742 (2006).
33. Solinas, G., Naugler, W., Galimi, E., Lee, M. S. & Karin, M. Saturated fatty acids inhibit induction of insulin gene transcription by JNK-mediated phosphorylation of insulin-receptor substrates. *Proceedings of the National Academy of Sciences of the United States of America* **103**, 16454–16459, doi: 10.1073/pnas.0607626103 (2006).
34. Jaeschke, A. & Davis, R. J. Metabolic stress signaling mediated by mixed-lineage kinases. *Molecular cell* **27**, 498–508, doi: 10.1016/j.molcel.2007.07.008 (2007).
35. Li, Y. *et al.* Hepatic overexpression of SIRT1 in mice attenuates endoplasmic reticulum stress and insulin resistance in the liver. *FASEB J* **25**, 1664–1679, doi: 10.1096/fj.10-173492 [pii]10.1096/fj.10-173492 (2011).
36. Ji, C. Dissection of endoplasmic reticulum stress signaling in alcoholic and non-alcoholic liver injury. *Journal of gastroenterology and hepatology* **23** Suppl 1, S16–S24, doi: 10.1111/j.1440-1746.2007.05276.x (2008).
37. Sreejayan, N., Dong, F., Kandadi, M. R., Yang, X. & Ren, J. Chromium alleviates glucose intolerance, insulin resistance, and hepatic ER stress in obese mice. *Obesity* **16**, 1331–1337, doi: 10.1038/oby.2008.217 (2008).
38. Qiu, W., Su, Q., Rutledge, A. C., Zhang, J. & Adeli, K. Glucosamine-induced endoplasmic reticulum stress attenuates apolipoprotein B100 synthesis via PERK signaling. *Journal of lipid research* **50**, 1814–1823, doi: 10.1194/jlr.M800343-JLR200 (2009).
39. Lisbona, F. *et al.* BAX inhibitor-1 is a negative regulator of the ER stress sensor IRE1alpha. *Molecular cell* **33**, 679–691, doi: 10.1016/j.molcel.2009.02.017 (2009).
40. Zong, H., Armoni, M., Harel, C., Karnieli, E. & Pessin, J. E. Cytochrome P-450 CYP2E1 knockout mice are protected against high-fat diet-induced obesity and insulin resistance. *American journal of physiology. Endocrinology and metabolism* **302**, E532–E539, doi: 10.1152/ajpendo.00258.2011 (2012).
41. Abdelmegeed, M. A. *et al.* Critical role of cytochrome P450 2E1 (CYP2E1) in the development of high fat-induced non-alcoholic steatohepatitis. *Journal of hepatology* **57**, 860–866, doi: 10.1016/j.jhep.2012.05.019 (2012).
42. Kathirvel, E., Morgan, K., French, S. W. & Morgan, T. R. Overexpression of liver-specific cytochrome P4502E1 impairs hepatic insulin signaling in a transgenic mouse model of nonalcoholic fatty liver disease. *European journal of gastroenterology & hepatology* **21**, 973–983, doi: 10.1097/MEG.0b013e328328f461 (2009).
43. Bloch-Damti, A. & Bashan, N. Proposed mechanisms for the induction of insulin resistance by oxidative stress. *Antioxidants & redox signaling* **7**, 1553–1567, doi: 10.1089/ars.2005.7.1553 (2005).
44. Montgomery, M. K. & Turner, N. Mitochondrial dysfunction and insulin resistance: an update. *Endocrine connections* **4**, R1–R15, doi: 10.1530/EC-14-0092 (2015).
45. Kim, J. A., Wei, Y. & Sowers, J. R. Role of mitochondrial dysfunction in insulin resistance. *Circulation research* **102**, 401–414, doi: 10.1161/CIRCRESAHA.107.165472 (2008).
46. Ren, L. P. *et al.* Differing endoplasmic reticulum stress response to excess lipogenesis versus lipid oversupply in relation to hepatic steatosis and insulin resistance. *PLoS one* **7**, e30816, doi: 10.1371/journal.pone.0030816 (2012).
47. Hoffmann, C. *et al.* From endoplasmic reticulum to mitochondria: absence of the Arabidopsis ATP antiporter endoplasmic Reticulum Adenylate Transporter1 perturbs photorespiration. *The Plant cell* **25**, 2647–2660, doi: 10.1105/tpc.113.113605 (2013).
48. Marchi, S., Patergnani, S. & Pinton, P. The endoplasmic reticulum-mitochondria connection: one touch, multiple functions. *Biochimica et biophysica acta* **1837**, 461–469, doi: 10.1016/j.bbabi.2013.10.015 (2014).
49. Sivitz, W. I. & Yorek, M. A. Mitochondrial dysfunction in diabetes: from molecular mechanisms to functional significance and therapeutic opportunities. *Antioxidants & redox signaling* **12**, 537–577, doi: 10.1089/ars.2009.2531 (2010).
50. Rains, J. L. & Jain, S. K. Oxidative stress, insulin signaling, and diabetes. *Free radical biology & medicine* **50**, 567–575, doi: 10.1016/j.freeradbiomed.2010.12.006 (2011).
51. Zhou, H. & Liu, R. ER stress and hepatic lipid metabolism. *Frontiers in genetics* **5**, 112, doi: 10.3389/fgene.2014.00112 (2014).
52. Caro, A. A. & Cederbaum, A. I. Oxidative stress, toxicology, and pharmacology of CYP2E1. *Annual review of pharmacology and toxicology* **44**, 27–42, doi: 10.1146/annurev.pharmtox.44.101802.121704 (2004).
53. Caro, A. A. & Cederbaum, A. I. Role of phosphatidylinositol 3-kinase/AKT as a survival pathway against CYP2E1-dependent toxicity. *The Journal of pharmacology and experimental therapeutics* **318**, 360–372, doi: 10.1124/jpet.106.102921 (2006).
54. Kathirvel, E., Chen, P., Morgan, K., French, S. W. & Morgan, T. R. Oxidative stress and regulation of anti-oxidant enzymes in cytochrome P4502E1 transgenic mouse model of non-alcoholic fatty liver. *Journal of gastroenterology and hepatology* **25**, 1136–1143, doi: 10.1111/j.1440-1746.2009.06196.x (2010).
55. Schattenberg, J. M., Wang, Y., Singh, R., Rigoli, R. M. & Czaja, M. J. Hepatocyte CYP2E1 overexpression and steatohepatitis lead to impaired hepatic insulin signaling. *The Journal of biological chemistry* **280**, 9887–9894, doi: 10.1074/jbc.M410310200 (2005).
56. Dey, A., Kessova, I. G. & Cederbaum, A. I. Decreased protein and mRNA expression of ER stress proteins GRP78 and GRP94 in HepG2 cells over-expressing CYP2E1. *Archives of biochemistry and biophysics* **447**, 155–166, doi: 10.1016/j.abb.2006.01.013 (2006).
57. Lewis, M. D. & Roberts, B. J. Role of CYP2E1 activity in endoplasmic reticulum ubiquitination, proteasome association, and the unfolded protein response. *Archives of biochemistry and biophysics* **436**, 237–245, doi: 10.1016/j.abb.2005.02.010 (2005).
58. Howarth, D. L. *et al.* Alcohol disrupts endoplasmic reticulum function and protein secretion in hepatocytes. *Alcoholism, clinical and experimental research* **36**, 14–23, doi: 10.1111/j.1530-0277.2011.01602.x (2012).
59. Chen, K., Kirber, M. T., Xiao, H., Yang, Y. & Keaney, J. F. Jr. Regulation of ROS signal transduction by NADPH oxidase 4 localization. *The Journal of cell biology* **181**, 1129–1139, doi: 10.1083/jcb.200709049 (2008).

60. Frand, A. R. & Kaiser, C. A. Ero1p oxidizes protein disulfide isomerase in a pathway for disulfide bond formation in the endoplasmic reticulum. *Molecular cell* **4**, 469–477 (1999).
61. Fauconnier, J. *et al.* Effects of palmitate on Ca(2+) handling in adult control and ob/ob cardiomyocytes: impact of mitochondrial reactive oxygen species. *Diabetes* **56**, 1136–1142, doi: 10.2337/db06-0739 (2007).
62. Sprinzl, M. F., Oberwinkler, H., Schaller, H. & Protzer, U. Transfer of hepatitis B virus genome by adenovirus vectors into cultured cells and mice: crossing the species barrier. *Journal of virology* **75**, 5108–5118, doi: 10.1128/JVI.75.11.5108-5118.2001 (2001).
63. Park, J. S., Surendran, S., Kamendulis, L. M. & Morral, N. Comparative nucleic acid transfection efficacy in primary hepatocytes for gene silencing and functional studies. *BMC Res Notes* **4**, 8, doi: 10.1186/1756-0500-4-8 (2011).

Acknowledgements

This study was supported by grants (2015R1A2A1A13001849, 2008-0062279 (to H.J.C.), NRF-2015R1A2A1A01006687, NRF-2012M3A9B6055345, and NRF-2015R1A5A1009024 (to S.H.K)) from the National Research Foundation of Korea. HJC is also supported by a grant of the Korea Health technology R&D Project (grant no: A121931). SHK is also supported by a grant of the Korea Health technology R&D Project (grant no: HI13C1886), Ministry of Health & Welfare, Republic of Korea and a grant from Korea University, Seoul, Republic of Korea.

Author Contributions

H.-R.K. designed the experiment. G.-H.L., H.-Y.L., K.-J.O. and H.-S.H. conducted the experiments. H.-R.K., K.-G.P. and K.-H.N. preparation of manuscript. S.-H.K. and H.-J.C. supervised and participated in the data analysis and interpretation. All authors reviewed the manuscript.

Additional Information

Supplementary information accompanies this paper at <http://www.nature.com/srep>

Competing financial interests: The authors declare no competing financial interests.

How to cite this article: Lee, G.-H. *et al.* Effect of BI-1 on insulin resistance through regulation of CYP2E1. *Sci. Rep.* **6**, 32229; doi: 10.1038/srep32229 (2016).



This work is licensed under a Creative Commons Attribution 4.0 International License. The images or other third party material in this article are included in the article's Creative Commons license, unless indicated otherwise in the credit line; if the material is not included under the Creative Commons license, users will need to obtain permission from the license holder to reproduce the material. To view a copy of this license, visit <http://creativecommons.org/licenses/by/4.0/>

© The Author(s) 2016